THE ASTROPHYSICAL JOURNAL, 413:L15–L18, 1993 August 10

THE X-RAY BALDWIN EFFECT

KAZUSHI IWASAWA
Department of Astrophysics, Nagoya University, Chikusa-ku, Nagoya 464-01, Japan
AND
YOSHIAKI TANIGUCHI
Astronomical Institute, Tohoku University, Aoba, Sendai 980, Japan
Received 1993 March 15; accepted 1993 May 25

ABSTRACT

Using the X-ray data of active galactic nuclei (type 1 Seyfert galaxies and quasars) obtained by the X-ray satellite *Ginga*, we have found that the equivalent width of the Fe K emission line at 6.4 keV, EW(Fe K), is inversely correlated with the X-ray luminosity in the 2–10 keV band. This inverse correlation is basically similar to the well-known relation known as the "Baldwin effect," which means that the equivalent width of the C IV λ1550 emission line is inversely correlated with the UV continuum luminosity (Baldwin 1977). Hence, we may call our finding "the X-ray Baldwin effect." The X-ray Baldwin effect is pronounced for type 1 Seyfert galaxies. The obtained correlation, EW(Fe K) $\propto L_X(2\text{–}10\ \text{keV})^{-0.20\pm0.03}$, is quite similar to those of the original Baldwin effects for type 1 Seyfert galaxies and quasars, implying that the Fe K emission mainly comes from the broad-line regions or from the regions whose geometrical configurations are nearly the same as those of broad-line regions.

Subject headings: galaxies: Seyfert — quasars: emission lines — X-rays: galaxies

1. INTRODUCTION

The active galactic nuclei (AGNs) emit their energy in the wide range of frequency from radio through infrared, optical, ultraviolet, to X-ray and γ-ray. The photoionization by high-energy photons produced in the central engine is a source of heating and excitation for the surrounding gas, which is responsible for the X-ray absorption, emission, and/or reflection. Therefore, X-ray spectra have been used to study the physical natures of very close regions of AGNs. The most prominent line in the X-ray spectra of AGNs is Fe K fluorescence line emission. Since the pioneering detection of Fe K by Mushotzky (1982) from three Seyfert galaxies, NGC 2992, NGC 5506, and MCG 5-23-16, the Fe K emission has been observed in many AGNs (Matsuoka et al. 1986; Morini, Lipani, & Molteni 1987; Wang et al. 1986; Kunieda et al. 1990; Pounds et al. 1990; Piro, Yamauchi, & Matsuoka 1990), including quasars (Turner et al. 1990; Kii et al. 1991; Williams et al. 1992).

The origin of the Fe K emission has been discussed in terms of Compton reflection in an accretion disk (Lightman & White 1988; George & Fabian 1991; Matt, Perola, & Piro 1991) or partially covering dense clouds (Piro et al. 1990; Sivron & Tsuruta 1993; Netzer 1993). However, there is still a controversy on the origin of the Fe K emission from AGNs (cf. Kunieda et al. 1990; Weaver et al. 1992). In this *Letter*, in order to study the origin of Fe K emission from AGNs, we analyze published Fe K emission data of AGNs from a different point of view. That is, we examine how the Fe K equivalent widths are correlated with the X-ray continuum luminosities. This analysis is analogous to that of the Baldwin effect, i.e., the continuum luminosity dependence of the C IV λ1550 equivalent width (Baldwin 1977). We find the inverse correlation between the Fe K equivalent width and the X-ray (2–10 keV) luminosity, which is nearly the same trend as that shown in the Baldwin effect. We will discuss the nature of the Fe K emission in analogy to the analysis of the Baldwin effect.

2. DATA

We compiled the X-ray data of AGNs involving the energy of 6.4 keV because our primary purpose was to study Fe K emission properties. All the data are taken from literature based on the observations with *Ginga* (references are given in Table 1). It should be noted that most of the data on Seyfert galaxies are taken from Awaki et al. (1991), while most of the data on the quasars are from Table 3 of Williams et al. (1992). We include seven Seyfert galaxies and two quasars which have been newly analyzed using the *Ginga* archival data (Awaki 1993; this work). The reduction procedures are the same as that described in Awaki et al. (1991). The spectral fittings were performed using a model of a single power law modified by the low-energy absorption and Fe K edge and a narrow Gaussian line. That is, most of the X-ray spectra were reduced homogeneously with the same procedure. In this way, we collect the X-ray data for 37 AGNs (19 Seyferts and 18 quasars).

The sample is classified into the following two categories: (1) Seyfert galaxies and (2) quasars. The Seyfert sample contains 14 type 1, one type 1.5, and one type 1.8 Seyfert; one narrow-line X-ray galaxy (NLXG); and two broad-line radio galaxies (BLRGs). The quasar sample consists of nine radio-loud and nine radio-quiet quasars. The data are summarized in Table 1. Here we should note that most of the sample AGNs show a time variability in X-rays (continuum and Fe K emission) on the time scale from hours to about a year. For these AGNs, we take their mean values. For 3C 273, two observations are listed in Table 1B. One is taken in faint phase in which significant detection of Fe K was reported, and the other in bright phase. Finally, we note that type 2 Seyfert galaxies are not included in our sample because their Fe K emission mechanism is considered to be different from that of unobscured AGNs (cf. Koyama et al. 1989; Awaki et al. 1991).

The X-ray luminosities (2–10 keV) of our sample cover about five orders, in the range log L_X (ergs s^{-1}) $\simeq$ 41.7–47.2. Here the distances of the objects are estimated with use of a

Hubble constant $H_0 = 50$ km s^{-1} Mpc^{-1}. The mean energy indices between 3 and 20 keV are 0.74 ± 0.18 for the Seyfert galaxies and 0.74 ± 0.28 for the quasars. With small exceptions, the Seyfert sample shows a tight distribution of the X-ray slope close to the canonical value, $\alpha \sim 0.7$. In contrast, the quasar sample has a broader distribution in the spectral slope.

TABLE 1A

SEYFERT SAMPLE

Name (1)	α (2)	log L_X (3)	EW (4)	Reference (5)
NGC 3227	$0.63^{+0.02}_{-0.05}$	42.5	190 ± 50	1, 2
NGC 3516	$0.51^{+0.05}_{-0.04}$	43.0	220 ± 40	3, 4
NGC 4051	$0.97^{+0.04}_{-0.03}$	41.7	250 ± 50	5
NGC 4151	$0.55^{+0.07}_{-0.07}$	42.7	167 ± 25	6
NGC 4593	$0.64^{+0.03}_{-0.02}$	43.0	170 ± 30	3
NGC 5506	$0.82^{+0.05}_{-0.05}$	43.1	190 ± 30	2
NGC 5548	$0.64^{+0.01}_{-0.01}$	43.8	120 ± 20	3, 7
NGC 6814	$0.42^{+0.06}_{-0.06}$	42.8	330 ± 30	8
NGC 7469	$0.83^{+0.01}_{-0.01}$	43.7	150 ± 35	9
Mrk 335	$1.15^{+0.08}_{-0.08}$	43.8	155 ± 70	1, 10
Mrk 509	$0.70^{+0.02}_{-0.02}$	44.5	80 ± 40	1, 11
IC 4329A	$0.71^{+0.01}_{-0.01}$	44.2	100 ± 20	8
MCG −2-58-22	$0.70^{+0.04}_{-0.05}$	44.3	180 ± 80	1
MCG −6-30-15	$0.65^{+0.07}_{-0.06}$	43.3	130 ± 20	3, 12
Akn 120	$0.68^{+0.04}_{-0.04}$	44.3	100 ± 50	1, 9
IRAS 15091−2107	$0.75^{+0.06}_{-0.04}$	44.0	190 ± 40	3
IRAS 18325−5926	$1.12^{+0.05}_{-0.05}$	43.7	190 ± 30	13, 3
3C 382	$0.73^{+0.1}_{-0.1}$	44.3	160 ± 80	1, 14
3C 390.3	$0.74^{+0.01}_{-0.02}$	44.8	43 ± 20	1

TABLE 1B

QUASAR SAMPLE

Name (1)	α (2)	log L_X (3)	EW (4)	Reference (5)
PKS 0637−752	$0.83^{+0.16}_{-0.08}$	46.5	200 ± 165	15
PKS 0837−120	$0.89^{+0.36}_{-0.20}$	45.1	<300	15
PKS 1217+023	$0.49^{+0.20}_{-0.12}$	45.2	<290	15
3C 273 (low)	$0.53^{+0.02}_{-0.01}$	45.8	54 ± 27	15
3C 273 (high)	$0.53^{+0.01}_{-0.01}$	46.2	<31	15
3C 279	$0.67^{+0.04}_{-0.04}$	45.6	<100	16
4C 31.63	$0.69^{+0.15}_{-0.16}$	45.2	<450	15
4C 34.47	$0.64^{+0.17}_{-0.14}$	45.3	<120	17
NRAO 140	$0.72^{+0.11}_{-0.11}$	47.2	<200	17
PHL 1657	$0.81^{+0.06}_{-0.06}$	45.4	<140	15
PG 0026+129	$0.31^{+0.09}_{-0.09}$	44.9	<200	18
PG 0804+761	$1.08^{+0.12}_{-0.13}$	44.4	<530	15
PG 1211+143	$1.11^{+0.24}_{-0.17}$	44.5	<450	15
PG 1307+085	$0.86^{+0.16}_{-0.09}$	44.9	<280	15
PG 1416−129	$0.10^{+0.16}_{-0.09}$	44.7	<250	15
PG 1426+015	$0.66^{+0.10}_{-0.10}$	44.6	<200	18
II Zw 136	$1.29^{+0.32}_{-0.21}$	43.9	<600	15
Mrk 205	$0.91^{+0.09}_{-0.09}$	44.3	300 ± 200	15
E1821+643	$0.93^{+0.11}_{-0.08}$	46.0	60–380	19

Col. (2).—Energy index of the X-ray spectra typically in the 3–20 keV band (see text).

Col. (3).—Logarithmic X-ray luminosity in the 2–10 keV band, in units of ergs s^{-1}.

Col. (4).—Equivalent width of the Fe K emission line in units of eV.

REFERENCES.—(1) Awaki 1993; (2) Pounds et al. 1989; (3) Awaki et al. 1991; (4) Kolman et al. 1993; (5) Kunieda et al. 1992; (6) Yaqoob & Warwick 1991; (7) Nandra et al. 1991; (8) Kunieda et al. 1990; (9) Piro et al. 1990; (10) Pounds et al. 1990; (11) Singh et al. 1990; (12) Nandra et al. 1990; (13) Iwasawa et al. 1993; (14) Kaastra et al. 1991; (15) Williams et al. 1992; (16) Makino et al. 1989; (17) Ohashi et al. 1992; (18) this work; (19) Kii et al. 1991.

3. RESULTS

3.1. *Correlation between Equivalent Width of the* Fe K *Emission and X-Ray Luminosity*

In Figure 1 we show the correlation between the equivalent width of the Fe K emission [EW(Fe K)] and the X-ray luminosity (L_X) for the Seyfert galaxies and the quasars. It is clearly shown for the Seyfert galaxies that there is a good anticorrelation between EW(Fe K) and L_X. The linear fit to EW(Fe K) as a function of log L_X [i.e., EW(Fe K) $\propto$ log L_X], weighting with the observational uncertainties, results in a highly significant correlation coefficient (>0.8). Further, the power-law fit [EW(Fe K) $\propto L_X^{\gamma}$] also provides a statistically significant correlation, giving the best-fit power index of $\gamma = -0.20 \pm 0.03$. The fitting results are summarized in Table 2.

Within the uncertainties, the relationship found in the Seyfert sample can be extended to the quasar sample. However, because of poor constraints, we cannot conclude that the relationship is true for all quasars. At least for the positively Fe K detected objects in both the Seyfert and the quasar sample, a significant correlation with the same trend can be seen (see Table 2). Future higher sensitivity X-ray spectroscopy will be necessary to discuss this important problem.

3.2. *Comments on Individual Objects*

Time variability in X-rays is one of the important characteristics of AGNs. In this subsection we give comments on the relation between the Fe K strengths and the variable X-ray continuum for two Seyfert galaxies, NGC 4151 and NGC 6814.

1. *NGC 4151.*—Yaqoob & Warwick (1991) published the X-ray data in the time span of 20 months. Analyzing their data, we find a remarkably clear inverse correlation between EW(Fe K) and L_X, but a very steep relationship [EW(Fe K) $\propto L_X^{-1.26 \pm 0.16}$]. The lack of a response of the Fe K flux to the continuum variation produced the inverse correlation.

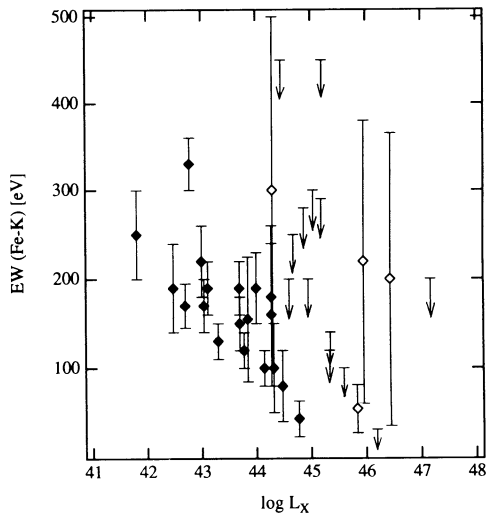

FIG. 1.—Relation between the Fe K equivalent width [EW(Fe K)], in units of eV, and the logarithmic X-ray luminosity (L_X) in the 2–10 keV band, in units of ergs s^{-1}. The Seyfert galaxies and the quasars are denoted by filled diamonds and open diamonds, respectively. The symbols with an arrow show the upper-limit data.

TABLE 2

EQUIVALENT WIDTH OF Fe K VERSUS X-RAY LUMINOSITY CORRELATIONS

	EW $\propto a \log L_X$			EW $\propto L_X^{\gamma}$	
SAMPLE (1)	n (2)	a (3)	R (4)	γ (5)	R (6)
1. Seyferts	19	-77 ± 15	0.83	-0.20 ± 0.04	0.80
2. Seyferts + quasar	23	-68 ± 11	0.81	-0.20 ± 0.03	0.82

Col. (1).—(1) All Seyfert galaxies in Table 1A. The Fe K lines are positively detected in them. (2) This sample is composed of AGNs in sample 1 and quasars with positive detection of the Fe K.

Col. (2).—Number of AGNs in sample.

Cols. (3) and (5).—Best-fit values for a and γ in the equations that are given above, derived from weighting least-squares fit.

Cols. (4) and (6).—Correlation coefficients of the relationship.

2. *NGC 6814.*—This galaxy is quite unique for both the unusually large EW(Fe K) and the rapid variability of the continuum and the Fe K line (Kunieda et al. 1990). The line flux linearly responds to the continuum variation. Hence, there is no individual X-ray Baldwin effect in this galaxy.

The X-ray Baldwin effect in an *individual* object might be an effect of a difference in time variability between the line and the continuum flux. However, it cannot be the cause of the global X-ray Baldwin effect found for the sample AGNs, because of the localized L_X compared with the L_X range for the sample. The different behaviors in global and individual data may not be serious but may be separate problems originating from separate causes.

4. DISCUSSION

4.1. *The X-Ray Baldwin Effect*

The inverse correlation between EW(Fe K) and L_X found in this study is quite similar to the well-known correlation called "the Baldwin effect." Taking account of the similarity, we hereafter refer to the inverse correlation between EW(Fe K) and L_X as "the X-ray Baldwin effect."

It is generally considered that the Fe K line in AGNs is mainly produced via fluorescence. If the X-ray continuum spectrum and the fluorescence yield are similar from object to object, it is natural to consider that EW(Fe K) depends on the covering factor and the optical depth (e.g., Blandford 1990). The absorbing column along the line of sight measured by the low-energy absorption is insufficient to account for the observed EW(Fe K). There are two alternative interpretations for this phenomenon. One is that the Fe K reprocessor of optically thick material (e.g., an accretion disk or a molecular/dust torus) is located out of the line of sight (cf. Fabian et al. 1989; George & Fabian 1991; Awaki et al. 1991). The other is that the central engine is partially covered by cold or photoionized clouds (Holt et al. 1980; Halpern 1984; Piro et al. 1990; Yaqoob & Warwick 1991; Netzer 1993). Although these models describe the place where the Fe K line arises, they are not able to predict the X-ray Baldwin effect straightforwardly.

A thin accretion disk model proposed by Netzer (1985) can explain the original Baldwin effect naturally because the difference in aspect dependence between the UV continuum and the C IV line emission is introduced in the model. However, if the X-ray Fe K emission also arises from the accretion disk, one cannot explain the X-ray Baldwin effect. Alternatively, we propose a tentative explanation. Assuming that the anisotropy of the primary emission increases with increasing X-ray luminosity in AGNs and that the geometry of the Fe K reprocessor is similar from object to object, we can observe the X-ray Baldwin effect. This idea will be open to question.

If the covering factor of the Fe K emitting regions depends on the X-ray luminosity of the central engine, we may expect the X-ray Baldwin effect. Such a model was proposed by Mushotzky & Ferland (1984) to explain the original Baldwin effect. They introduced the luminosity-dependent covering factor (Ω) as well as ionization parameter, and showed the luminosity dependence of the covering factor as $\Omega \propto L^{-0.2}$, consistent with our X-ray Baldwin effect for the type 1 Seyfert galaxies. This dependence is also consistent with both the original Baldwin relationship for the type 1 Seyfert galaxies (Wu, Boggess, & Gull 1983) and the revised Baldwin relationship for quasars (Baldwin, Wampler, & Gaskell, 1989; Kinney, Rivolo, & Koratkar 1990). Thus the luminosity-dependent covering factor model (Mushotzky & Ferland 1984) successfully explains the X-ray Baldwin effect as well as the original Baldwin effect. The Fe K behaviors in quasars are still an issue for further investigation.

4.2. *The* Fe K *Emitting Regions*

The X-ray Baldwin effect discovered here is nearly identical to the original Baldwin effect. Since the C IV λ1550 emission comes from the broad-line regions (BLRs) photoionized by power-law continuum radiation, the similar Baldwin effects in both C IV and Fe K emission lines strongly suggest that Fe K emission mainly arises from the BLRs or from the regions whose geometrical configurations are nearly the same as those of BLRs.

The Fe K line profile would be crucial in the study of the location where the emission line arises. Unfortunately, since the spectral resolution of the *Ginga* large area counter (LAC) is very poor ($E/\Delta E \sim 5$ at the Fe K band; Turner et al. 1989), we can only get quite rough information about the line profile. While Yaqoob & Warwick (1991) gave FWHM(Fe K) $\simeq$ 38,000 km s^{-1}, the recent broad-band X-ray telescope (BBXRT) observations of NGC 4151 by Weaver et al. (1992) showed that the major component of the Fe K line shows FWHM(Fe K) $<$ 7500 km s^{-1}, and an underlying weak, broad component is present. Further, the width of the narrow Fe K line is comparable to FWHM(C IV) = 7600 $\pm$ 500 km s^{-1}, which was obtained at the same epoch, providing strong evidence that the Fe K emission arises from the BLR in NGC 4151. The lack of variability in Fe K flux corresponding to the continuum (Yaqoob & Warwick 1991; Weaver et al. 1992) suggests that the emission-line region is $\sim$2 light-years away from the continuum source or that it is under the matter-bounded condition.

In NGC 4151 the BLR clouds are predominantly neutral, and they are thought to be responsible for the variable X-ray absorption (Barr et al. 1977; Mushotzky, Holt, & Serlemitsos 1978; Yaqoob, Warwick, & Pounds 1989; Yaqoob & Warwick 1991). Therefore, the matter-bounded Fe K reprocessor is also plausible, being distinct from the BLRs, since hydrogen atoms are fully ionized in such gas, being optically thin in the X-ray continuum. It is consistent with the "very broad line region" which is thought to lie between the ionizing continuum and the BLR, and to be the X-ray photoionized absorber (Ferland, Korista, & Peterson 1990). This interpretation may explain both the FWHM(Fe K) of 38,000 km s^{-1} observed by *Ginga* (Yaqoob & Warwick 1991) and the broad component seen in the BBXRT spectrum (Weaver et al. 1992).

On the other hand, we have to be aware that the rapid response of the Fe K line flux to the continuum variations was observed, for example, in NGC 6814 (Kunieda et al. 1990). The time lag is less than 256 s, suggesting that the distance between the continuum source and the Fe K emitting region is less than $\sim 10^{13}$ cm. In this case, it is natural to consider that the Fe K emission arises in the radiation-bounded matter located very close to the central source.

We may summarize our conclusions as follows. The location of Fe K emitting regions is inferred to be in the wide range extending from near the central source ($\sim 10^{13}$ cm) to the BLRs ($\sim 10^{17}$–10^{18} cm), and different physical conditions from object to object are also suggested. We consider that AGNs may have the combination of Fe K lines from these distinct components. However, the X-ray Baldwin effect strongly suggests that the geometry of the primary Fe K emitter is similar to those of the BLRs.

We would like to thank Hisamitsu Awaki and Hideyo Kunieda for warm encouragement and useful discussion.

REFERENCES

Awaki, H. 1993, private communication
Awaki, H., Koyama, K., Inoue, H., & Halpern, J. P. 1991, PASJ, 43, 195
Baldwin, J. A. 1977, ApJ, 214, 679
Baldwin, J. A., Wampler, E. J., & Gaskel, C. M. 1989, ApJ, 338, 630
Barr, P., White, N., Sanford, P., & Irves, J. 1977, MNRAS, 181, 43P
Blandford, R. D. 1990, in Active Galactic Nuclei, ed. T. J.-L. Courvoiser & M. Mayor (Berlin: Springer-Verlag), 191
Fabian, A. C., Rees, M. J., Stella, L., & White, N. E. 1989, MNRAS, 238, 729
Ferland, G. J., Korista, K. T., & Peterson, B. M. 1990, ApJ, 363, L21
George, I. M., & Fabian, A. C. 1991, MNRAS, 249, 352
Halpern, J. P. 1984, ApJ, 218, 90
Holt, S. S., Mushotzky, R. F., Becker, R., Boldt, E., Serlemitsos, P., Szymkowiak, A., & White, N. 1980, ApJ, 241, L13
Iwasawa, K., Awaki, H., Kunieda, H., Tawara, Y., Koyama, K., Taniguchi, Y., & Murayama, T. 1993, in preparation
Kaastra, J. S., Awaki, H., & Kunieda, H. 1991, A&A, 242, 27
Kii, T., et al. 1991, ApJ, 367, 455
Kinney, A. L., Rivolo, A. R., & Koratkar, A. P. 1990, ApJ, 357, 338
Kolman, M., Halpern, J. P., Awaki, H., & Koyama, K. 1993, ApJ, 403, 592
Koyama, K., Inoue, H., Tanaka, Y., Awaki, H., Takano, S., Ohashi, T., & Matsuoka, M. 1989, PASJ, 41, 731
Kunieda, H., Hayakawa, S., Tawara, Y., Koyama, K., Tsuruta, S., & Leighly, K. 1992, ApJ, 384, 482
Kunieda, H., Turner, T. J., Awaki, H., Koyama, K., Mushotzky, R., & Tsusaka, Y. 1990, Nature, 345, 786
Lightman, A. P., & White, T. R. 1988, ApJ, 335, 57
Makino, F., et al. 1989, ApJ, 347, L9
Matsuoka, M., Ikegami, T., Inoue, H., & Koyama, K. 1986, PASJ, 38, 285
Matt, G., Perola, G. C., & Piro, L. 1991, A&A, 247, 25
Morini, M., Lipani, N. A., & Molteni, D. 1987, ApJ, 317, 145
Mushotzky, R. F. 1982, ApJ, 256, 92
Mushotzky, R., & Ferland, G. J. 1984, 278, 558
Mushotzky, R., Holt, S. S., & Serlemitsos, P. J. 1978, ApJ, 225, L115
Nandra, K., Pounds, K. A., & Stewart, G. C. 1990, MNRAS, 242, 660
Nandra, K., Pounds, K. A., Stewart, G. C., George, I. M., Hayashida, K., Makino, F., & Ohashi, T. 1991, MNRAS, 248, 760
Netzer, H. 1985, MNRAS, 216, 63
———. 1993, ApJ, 411, 594
Ohashi, T., Makishima, K., Kii, T., Makino, F., Turner, M. J. L., & Williams, O. R. 1992, ApJ, 398, 87
Piro, L., Yamauchi, M., & Matsuoka, M. 1990, ApJ, 360, L35
Pounds, K. A., Nandra, K., Stewart, G. C., George, I. M., & Fabian, A. C. 1990, Nature, 344, 132
Pounds, K. A., Nandra, K., Stewart, G. C., & Leighly, K. 1989, MNRAS, 240, 769
Singh, K. P., Westergaard, N. J., Schnopper, H. W., Awaki, H., & Tawara, Y. 1990, ApJ, 363, 131
Sivron, R., & Tsuruta, S. 1993, ApJ, 402, 420
Turner, M. J. L., et al. 1989, PASJ, 41, 345
Turner, M. J. L., et al. 1990, MNRAS, 244, 310
Wang, B., Inoue, H., Koyama, K., Tanaka, Y., Hirano, T., & Nagase, F. 1986, PASJ, 38, 685
Weaver, K. A., et al. 1992, ApJ, 401, L11
Williams, O. R., et al. 1992, ApJ, 389, 157
Wu, C.-C., Boggess, A., & Gull, T. R. 1983, ApJ, 266, 28
Yaqoob, T., & Warwick, R. S. 1991, MNRAS, 248, 773
Yaqoob, T., Warwick, R. S., & Pounds, K. A. 1989, MNRAS, 236, 153